

The micro-macro mechanics of granular materials

Stefan Luding

Particle Technology, DelftChemTech, TU Delft,
Julianalaan 136, 2628 BL Delft, The Netherlands
e-mail: s.luding@tnw.tudelft.nl

Abstract

Using discrete element method (DEM) simulations, it is possible to examine the evolution of dense granular materials during deformation. The approach includes both normal and tangential forces at the contacts, so that rotations of the particles are important due to friction. Several examples are presented, involving the formation of shear bands and the propagation of sound waves in non-cohesive granular packings.

The ultimate goal is to obtain from such 'microscopic' simulations the macroscopic constitutive laws that describe the material behavior in the framework of a continuum theory.

Introduction

One of today's great challenges in material science, mechanics and physics is the understanding and description of the material behavior under large deformations. For dry, non-cohesive granular media, the discrete element method is a convenient tool to gain insight into the evolution of localized shear bands that typically occur during shear deformations. Granular media are inhomogeneous, non-linear, disordered, and an-isotropic on a "microscopic" scale [1-3], where microscopic is to be understood as the grain size dimension. The irregular, random packing and the consequent inhomogeneous and an-isotropic stress distribution (that involves also large fluctuations of contact forces) are accompanied by a reorganization of the contact-network during deformation. If an initially isotropic contact network is deformed, the result can be an-isotropic in structure. If the structure of the network reaches its limit of stability, shear band localization is observed. Two examples of systems, where shear bands form, are given in the following.

On the other hand, small (periodic) perturbations propagate in a peculiar way through the system and involve longitudinal, shear, but possibly also rotational waves. One example of a longitudinal wave in an isotropic, inhomogeneous three-dimensional sample is given.

Discrete Element Model

The elementary units of granular materials are 'mesoscopic' grains, which deform under stress. Since the realistic modeling of the deformations of the particles is much too complicated, the interaction force is related to the overlap Δ of two particles, see Fig. 1. Since the evaluation of the inter-particle forces based on the overlap may not be sufficient to account for the inhomogeneous stress distribution inside the particles, our results are of the same quality as the assumptions made about the force-overlap relation. Two particles interact only if they are in contact, and the force between two particles is decomposed into a normal and a tangential part. For the sake of simplicity, we restrict ourselves to spherical particles here. The normal force is, in the simplest case, a linear spring that takes care of repulsion, and a linear dashpot that accounts for dissipation during contact. The tangential force involves dissipation due to Coulomb friction, but also some tangential elasticity that

allows for stick-slip behavior on the contact level [4,9,10]. Non-spherical particles like, e.g., polygons were also used recently [10] and micro-macro transition procedures have been developed [6-11] with the goal to understand the macroscopic material behavior on microscopic foundations.

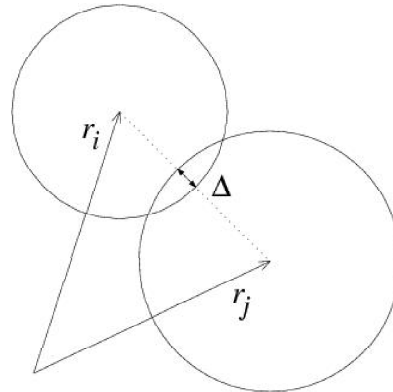


Figure 1 Two particle contact with overlap Δ

If all forces acting on a selected particle (either from other particles, from boundaries or from external forces) are known, the problem is reduced to the integration of Newton's equations of motion for the translational and rotational degrees of freedom:

$$m_i \frac{d^2}{dt^2} \mathbf{r}_i = \mathbf{f}_i + m_i \mathbf{g} \quad \text{and} \quad I_i \frac{d^2}{dt^2} \varphi_i = \mathbf{t}_i ,$$

with the gravitational acceleration \mathbf{g} , mass m_i of the particle, its position \mathbf{r}_i , the total force $\mathbf{f}_i = \sum_c \mathbf{f}_i^c$, acting on it due to contacts with other particles or with the walls, its moment of inertia I_i , its angular velocity $\boldsymbol{\omega}_i = d\varphi_i/dt$, and the total torque $\mathbf{t}_i = \sum_c \mathbf{l}_i^c \times \mathbf{f}_i^c$, with the center-contact "branch" vector \mathbf{l}_i^c .

Example 1: Two-dimensional simulations of a Bi-Axial Box

One possibility to gain insight into the material behavior of a granular packing is to perform elementary tests in the laboratory. Here, we chose as alternative the simulation with the discrete element model [4-10]. The set-up chosen for the two-dimensional numerical "experiment" is the bi-axial box, see Fig. 2, where the left and bottom walls are fixed. Stress- or strain-controlled deformation is applied to the side- and top-walls, respectively. In a typical simulation, the top wall is slowly shifted downwards, while the right wall moves, controlled by a constant stress p_x , responding on the forces exerted on it by the material in the box. The motion of the top-wall follows a cosine function, in order to allow for a smooth start-up and finish of the motion so that shocks and inertia effects are reduced, however, the shape of the function is arbitrary as long as it is smooth.

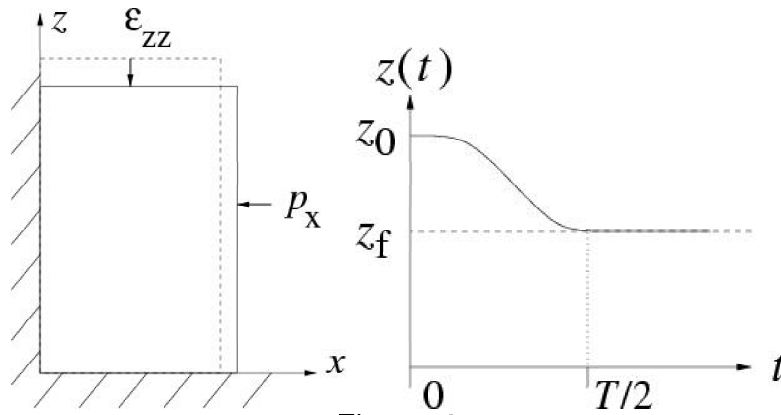


Figure 2

(Left) Schematic drawing of the model system. (Right) Position of the top-wall as function of time for the strain-controlled situation

The system examined in the following contains $N=1950$ particles with radii randomly drawn from a homogeneous distribution with minimum 0.5 mm and maximum 1.5 mm. The total mass of the particles in the system is about 0.02 kg. If not explicitly mentioned, the material stiffness is $k=10^5$ N/m and contact-viscosity is 0.1 kg/s. The eigenfrequency of the particle contact is hence typically 10^{-5} s so that an integration time-step of $2 \cdot 10^{-7}$ s is used, in order to allow for a “safe” integration [1]. The friction coefficient used later in the two-dimensional simulations is $\mu=0.5$, whereas the presented three-dimensional simulations are frictionless.

Stresses

Initially, the particles are randomly distributed in a huge box, with rather low overall density. Then the box is compressed, either by moving the walls to their desired position, or by defining an external pressure p , in order to achieve an isotropic initial condition. Starting from this relaxed, isotropic initial configuration, the strain ϵ_{zz} is applied to the top wall and the response of the system is examined. In Fig. 3, the volume change of a typical simulation shows first compression, then dilatancy, and eventually a very weak change at large deformations. At the same time, the stress response (xx and zz denote horizontal and vertical stresses, respectively) becomes more and more an-isotropic, i.e., the vertical stress increases strongly until it reaches a maximum. After the peak, softening behavior is evidenced with a constant, fluctuating stress for large deformations. Representative snapshots from this simulation are shown in Fig. 4.

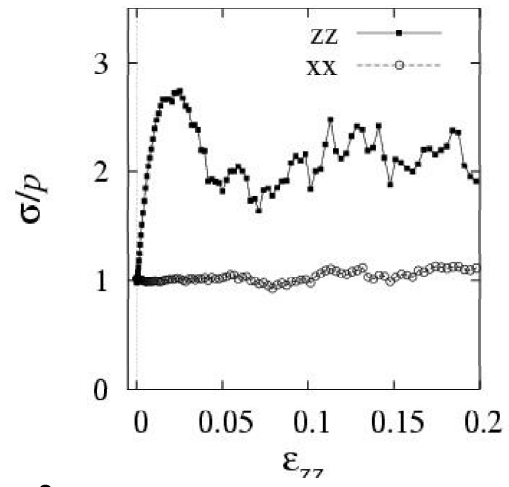
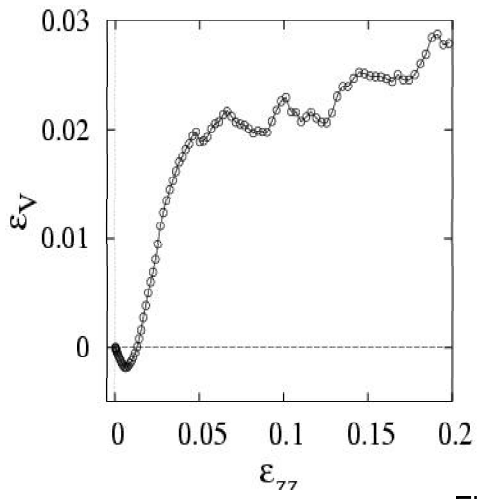
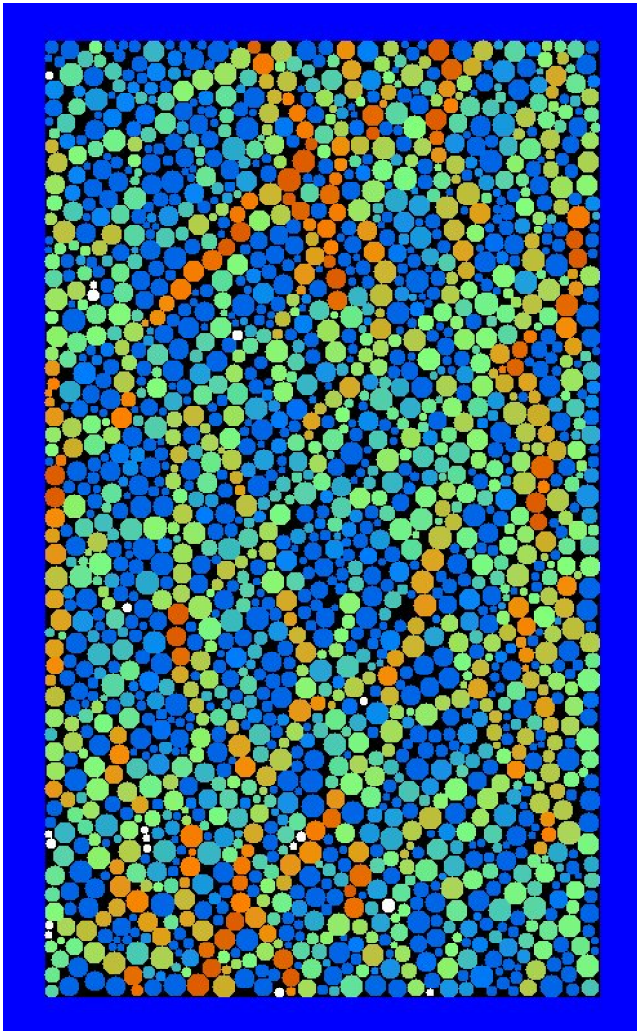


Figure 3
Volumetric strain (left) and stresses (right) during deformation



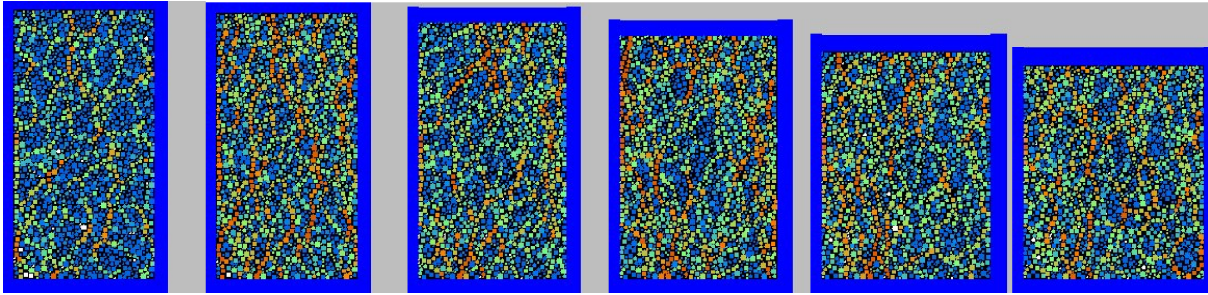


Figure 4

Snapshots of the simulation at different strains. The color-code corresponds to the potential contact-energy of each particle, decaying from red, green to blue. White particles are so-called “rattlers” and do not carry stress at all. The small pictures are taken at strains $\epsilon_{zz}=0.0027, 0.011, 0.042, 0.090, 0.151, 0.205$, the large one is a magnified version of the third at $\epsilon_{zz}=0.042$.

In the following pictures, snapshots from one simulation are shown and discussed with respect to different color-codes highlighting different interesting features of the granular material. As first example, in figure 4, the potential energy of the particles is shown, indicating the inhomogeneity of the forces and stresses. From one particle to the next, the stress (the potential energy density) can change by orders of magnitude. During the deformation, the so-called stress- or force-chains are formed and destroyed. This takes place with high probability in the direction against the applied deformation. With other words, the deformation causes an an-isotropic change of the (initially isotropic) structure, mainly acting against the direction of compression by creating new contacts. At the same time, in the perpendicular direction, contacts can open, until the structure is not stable anymore – shear-band localization is the consequence.

Deformations

A peculiar aspect of the system becomes evident when the displacement field in the center-of-mass reference frame is shown in Fig. 5. First, the deformation is isotropic, but at a larger deformation magnitude a shear band forms, breaking the overall symmetry of the system.

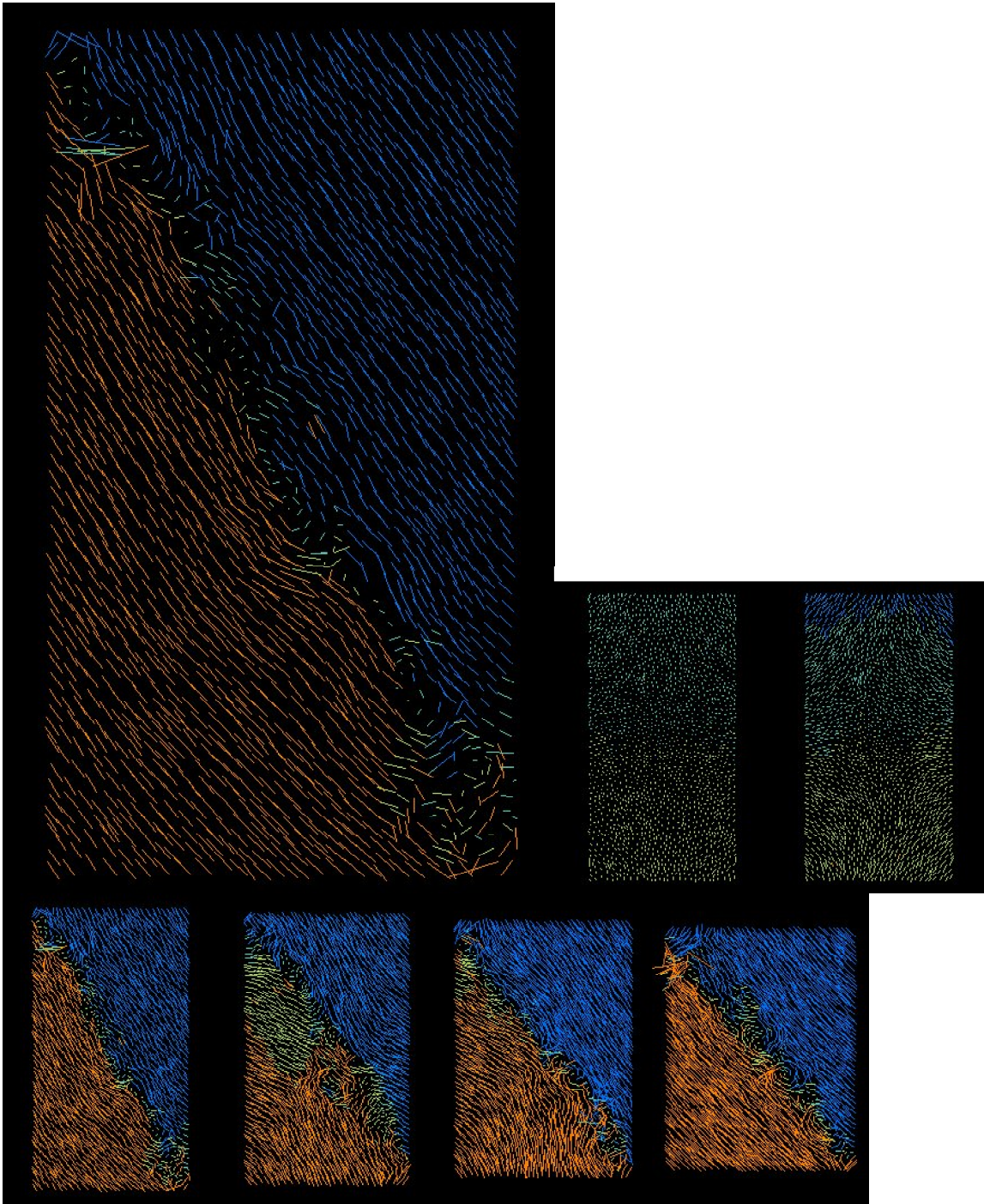


Figure 5

Snapshots of the simulation with the displacement field in the center of mass reference frame. Blue and red correspond to opposing directions of motion.

Rotations

The rotational motion of the particles is presented in Fig. 6. The particles rotate either clockwise (red) or counter-clockwise (blue) – or remain without rotation (green). Rotation is connected to shear displacement in the shear band, but the continuum-rotation caused by a shear deformation in the shear band is not the only rotation mode. In addition, the particles

have a peculiar eigen-rotation on top of the continuum mode. The material outside the shear band remains practically a solid block and rotations do not occur; only inside the dilated shear band rotations are possible. Note that the integrated field of strong rotations is much wider than the local shear bands due to the superposition of several more narrow shear-bands – one after the other.

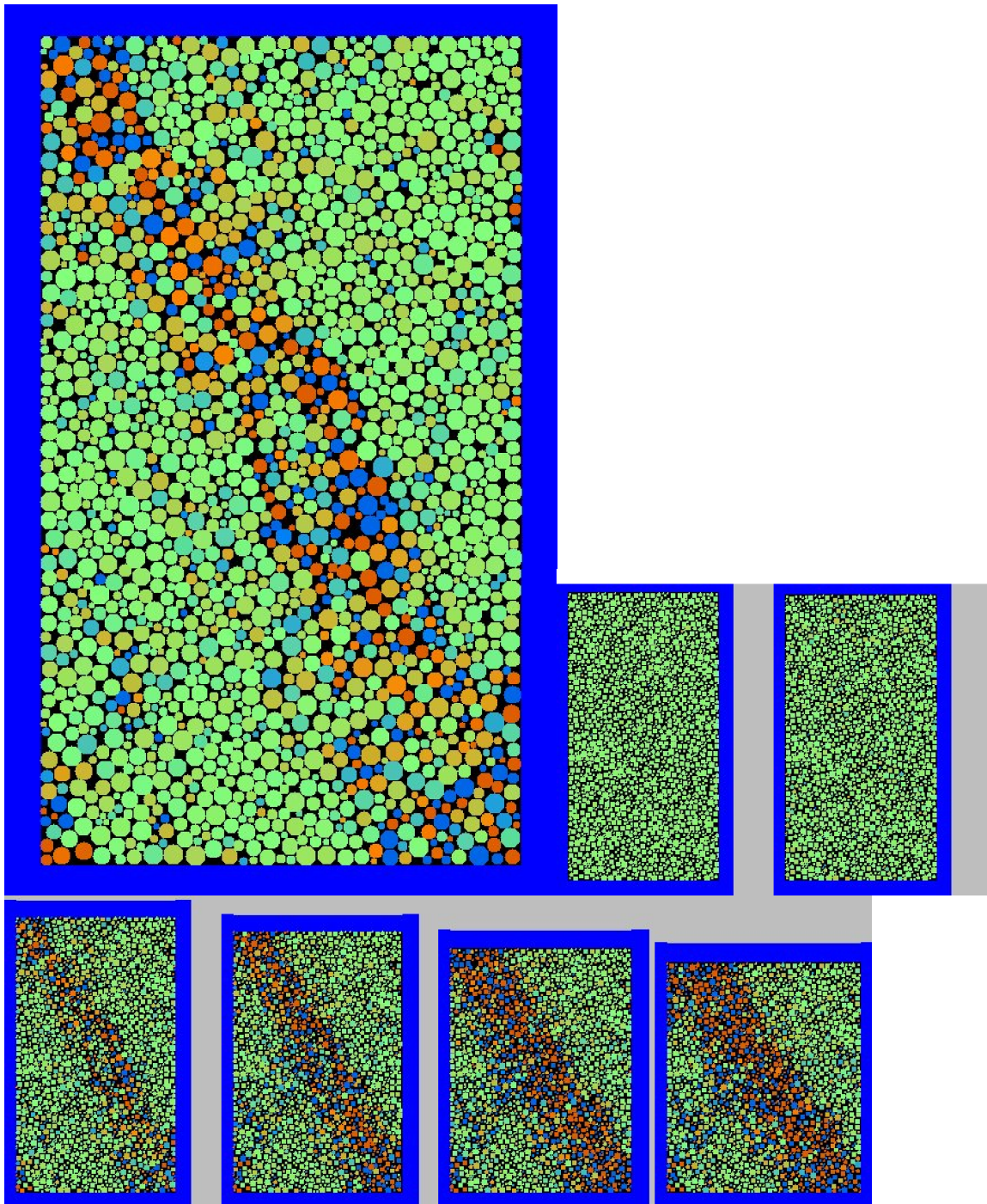


Figure 6

Snapshots with the integrated particle rotations color coded. This displays shear-band positions as well as the memory of the particles concerning their total rotation during the simulation

Micro-Macro Transition

Now it is possible to examine the flow behavior of the system by plotting Mohr-circles for the maximum stress (right-most point on the circle) for different confining pressures (left-most point), see Fig. 7. The tangent to these circles can be seen as the flow function for peak stress. It is linear for the examined parameters with a slope slightly larger than expected from the microscopic friction at the contacts alone. Since we have not used cohesive forces, the macroscopic cohesion is non-existent, i.e., the flow function hits the origin.

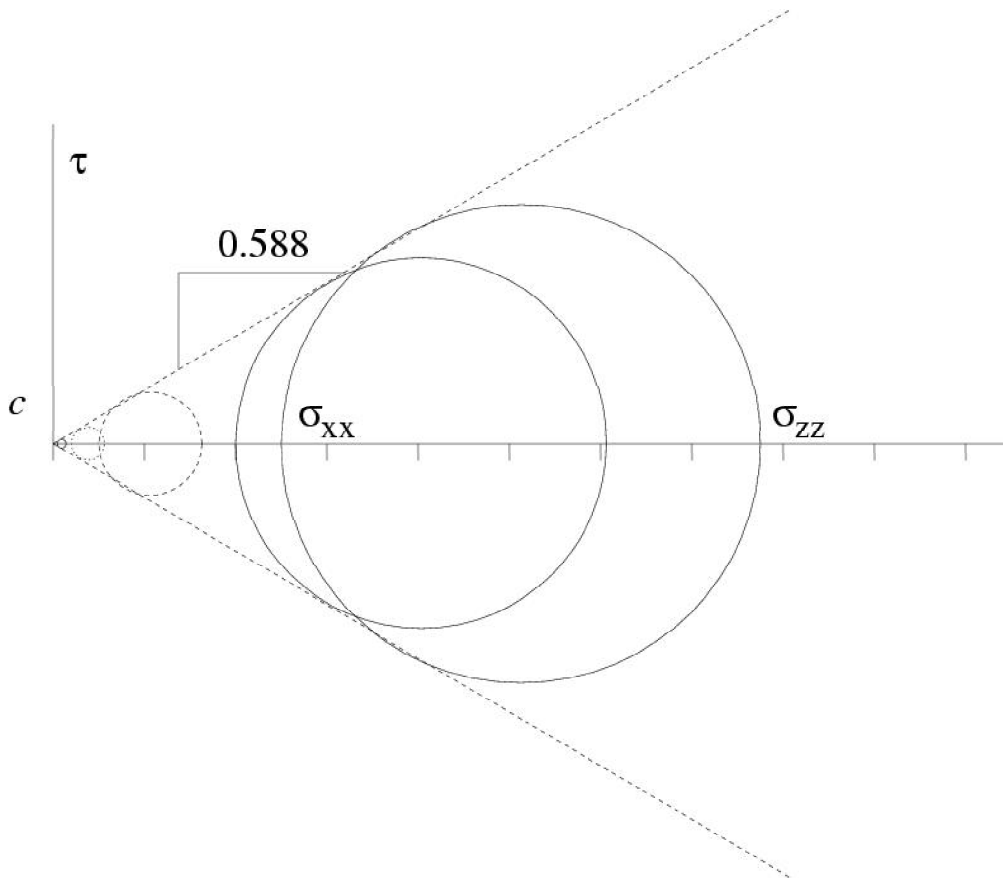


Figure 7

Mohr circle representation of the flow function at maximum stress

Example 2: Shear-cell in three dimensions

A special three-dimensional ring shear cell is shown as the next example in Figure 8. The system is a quarter of a cylindrical ring shear-cell with inner and outer wall radii 0.015 m and 0.110 m, respectively. The bottom wall consists of a disk with radius 0.085 m that is attached to the inner wall (static), and an outer flat ring that rotates with the outer wall. In order to enhance the roughness of the walls, about 10 percent of the particles are glued to the walls. The system (open to the top) is then filled with particles ranging from 0.75 mm to 1.5 mm in radius, to a height of about ten average particle diameters.

The slit at the bottom of the shear cell induces a shear band (transition region from red to blue in the right two pictures) with a width of about ten particle diameters. A more detailed study of the shear band formation for different filling heights as well as a comparison to experiments is in progress.

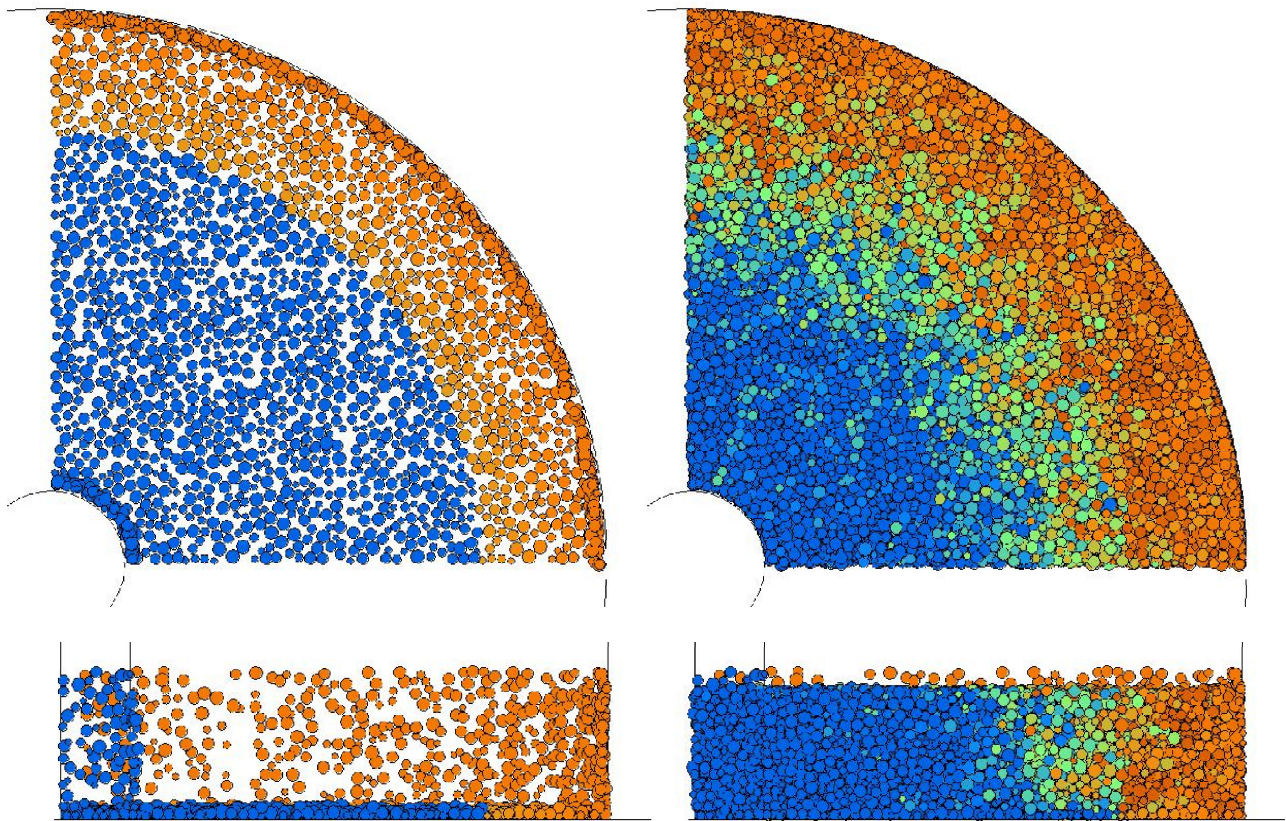


Figure 8

Snapshots (top-view and front-view) of a quarter of the ring shear cell, either empty (left) or filled with 22400 particles (right). The 2200 particles that can be seen in the left images are those glued to the bottom and the cylindrical walls (indicated by the lines). The inner wall and a fraction of the bottom are at rest (blue), while the outer wall with the remaining outer part of the bottom is rotating around the symmetry axis. Gravity acts in direction of view (top-) or vertically downward (bottom-pictures) and the color codes kinetic energy.

Example 3: Wave Propagation in a Static Packing

A simulation of a three-dimensional (3D) cuboid sample of 20000 spherical, polydisperse grains is presented next. The particle-particle interaction is the simplest possible linear spring-dashpot interaction on contact – tangential forces are neglected here. The sample can be viewed as an representative volume of, e.g., soil - deep underground with large confining pressure. It is subject to a longitudinal pulse agitated by an inwards motion of the left confining wall, see Fig. 9.

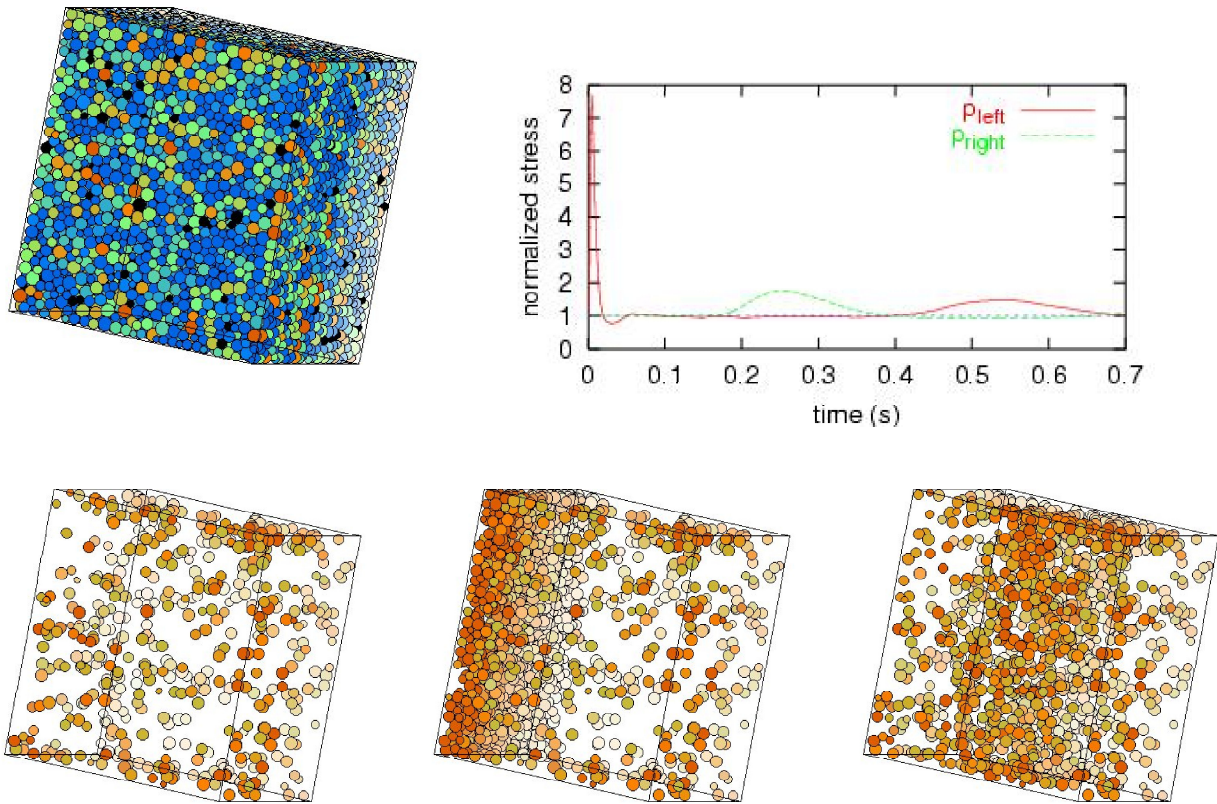


Figure 9

Snapshot of the cuboidal simulation volume (top-left) and the normal stress on left and right wall (top-right). Bottom: Wave propagation in the sample at times $t=0$ s, 0.02 s, and 0.14 s. The color code means: blue, green, red particles are under small, medium, and large stress. Note that only red particles under very high stress are plotted in the bottom pictures, showing the compressive P-wave.

The response wave arrives right, with a delay of about 0.2 s, with lower amplitude and strong dispersion (broadening) due to the linear interaction. In the next figure 10, the wave propagation is compared for two different types of interaction laws, namely the linear force-displacement used above and the Hertzian, non-linear spring, where the force is proportional to the deformation $\Delta^{3/2}$. In order to compare the shape of the waves, the data are appropriately rescaled with respect to the peak of the first-arrival on the side opposite to the initial pulse. The width of the Hertz-model wave is smaller than the width of the linear-model wave. More detailed studies concerning the effect of differences in particle sizes and the material properties are in progress.

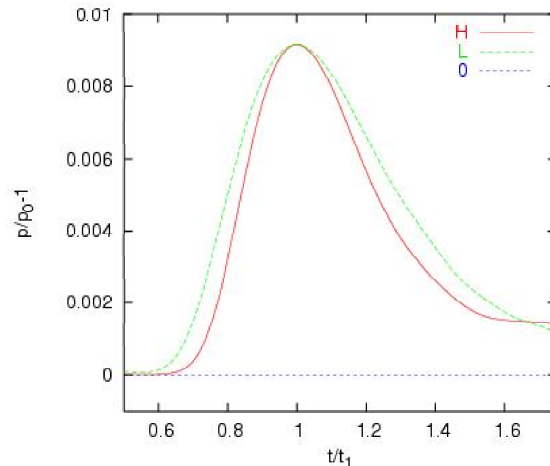


Figure 10

First arrival wave pressure signal (scaled by initial pressure and moved to 0) as function of time (scaled by the first-arrival wave peak time) at the target wall for a Hertz (H) and a Linear (L) contact law in the DEM simulation.

Summary

A discrete element simulation method was used for the microscopic modelling of dense, non-cohesive granular packings of round particles. Shear band formation was examined in two- and three-dimensional configurations, and the phenomenon of information (sound) propagation was studied.

In the first example, the biaxial box, anisotropy of the structure and the stress distribution during shear, is observed, but also strong inhomogeneities of forces and stresses, already in the initial isotropic situation are evidenced. During deformation, the stiffness and the anisotropy of the material increase until – going ahead with shear band localization – the material becomes softer and less an-isotropic. Eventually, a critical state shear regime is reached, where the properties of the material do not change any more – in average. Most of these features – and more – are also found in three-dimensional situations, as shown with two further examples.

Future work involves more detailed parameter studies, but also cohesive forces, both in two- and three-dimensional systems. The ultimate goal is to first quantitatively verify the simulation with experiments and then obtain constitutive relations from the model, based on the microscopic parameters used. A better microscopic insight and understanding also involves the development and use of micro-macro transition procedures [11] proposed for macroscopic fields like, e.g., deformation gradient or stress.

References

1. H. J. Herrmann, J.-P. Hovi, and S. Luding, eds., (1998) *Physics of dry granular media*, NATO ASI Series E 350, Kluwer Academic Publishers, Dordrecht.
2. P. A. Vermeer, S. Diebels, W. Ehlers, H. J. Herrmann, S. Luding, and E. Ramm, eds., (2001) *Continuous and Discontinuous Modelling of Cohesive Frictional Materials*, Lecture Notes in Physics 568, Springer, Berlin.

3. Y. Kishino, ed., (2001) *Powders & Grains 2001*, Balkema, Rotterdam.
4. P. A. Cundall and O. D. L. Strack, (1979), *A discrete numerical model for granular assemblies*, *Geotechnique* 29(1), 47—65.
5. Y.~M. Bashir and J.~D. Goddard, (1991), *A novel simulation method for the quasi-static mechanics of granular assemblages*, *J. Rheol.* 35(5), 849—885.
6. C.~Thornton, (2000), *Numerical simulations of deviatoric shear deformation of granular media*, *Geotechnique* 50(1), 43—53.
7. C.~Thornton and S.~J. Antony (2000), *Quasi-static deformation of a soft particle system*, *Powder Technology* 109(1-3), 179--191.
8. N.~P. Kruyt and L.~Rothenburg, (2001), *Statistics of the elastic behavior of granular materials*. *Int. J. of Solids and Structures* 38, 4879--4899.
9. M. Oda and K. Iwashita, (2000), *Study on couple stress and shear band development in granular media based on numerical simulation analyses*, *Int. J. of Engineering Science* 38, 1713-1740.
10. G. A. D'Addetta, F. Kun, E. Ramm, (2002), *On the application of a discrete model to the fracture process of cohesive granular materials*, *Granular Matter* 4 (2), 77-90.
11. S. Luding, M. Lätzel, W. Volk, S. Diebels, and H. J. Herrmann, (2001), *From discrete element simulations to a continuum model*, *Comp. Meth. Appl. Mech. Engng.* 191, 21-28.